Pharmaceutical Research, Vol. 7, No. 2, 1990

Research Article

DC Electrical Properties of Frozen, Excised Human Skin

Gerald B. Kasting[1,2] and Lisa A. Bowman[1]

Received April 20, 1989, accepted September 12, 1989

DC current–voltage relationships and sodium ion transport measurements for human allograft skin immersed in saline buffers have been determined using a four terminal potentiometric method and diffusion cells of our own design. About three-fourths of the skin samples were deemed suitable for study on the basis of their high resistivities and similar j–V characteristics. Most of these samples yielded sodium ion permeability coefficients less than or equal to those reported for human skin *in vivo*. The current–voltage relationship in these tissues was time dependent, highly nonlinear, and slightly asymmetric with respect to the sign of the applied potential. Skin resistance decreased as current or voltage increased. For current densities less than 15 $\mu A/cm^2$ and exposure times of 10–20 min, this decrease was almost completely reversible; at higher current densities, both reversible and irreversible effects were observed. The overall dependence of current on voltage was nearly exponential and was satisfactorily described by an equation of the form $j \sim \sinh V$. Diffusion potentials, sodium ion membrane transference numbers, and sodium ion flux enhancement factors during iontophoresis were measured for skin immersed both in normal saline solutions and in saline solutions of differing concentrations. The sign of the diffusion potentials and the value of the sodium ion transference number (0.51 in normal saline at pH 7.4) indicated a weak permselectivity of the skin for transport of sodium ion versus chloride. At a current density of 71 $\mu A/cm^2$ and transmembrane potentials in the range of 1.1–1.6 V, the flux enhancement for sodium ion was three to five times greater than that predicted for an uncharged homogeneous membrane according to electrodiffusion theory. For transmembrane potentials less than 0.17 V, agreement of this theory with the data was better but still incomplete.

KEY WORDS: iontophoresis; human skin; current–voltage characteristic; sodium ion transport.

INTRODUCTION

Electrically enhanced drug delivery through skin, or iontophoresis, has recently received increased attention as a means for systemic delivery of ionized drugs (1). The method has the potential to deliver transdermally drugs which were previously thought to be unsuitable due to poor skin penetration. The possibility of programmed delivery from an iontophoretic device makes such a device an attractive candidate (in theory, at least) for delivery of drugs requiring nonuniform delivery rates, e.g., small peptide hormones (1–3).

One quickly finds in the laboratory that, while it is possible to increase the skin penetration rates of many ionic compounds using iontophoresis, the efficiency with which this is accomplished is often not very high. Much of the electric current is carried by ions other than the drug ion of interest. In particular, the presence of substantial concentrations of sodium and chloride ions in the skin inevitably leads to a situation in which the drug ion competes as the charge carrier with one or the other of these small, relatively mobile ions (4). Since the total amount of current which can be passed through the skin is limited by the battery of the iontophoretic device and by the tolerance of the patient to the treatment, the efficiency of iontophoretic delivery becomes a key question in determining its practical value for a particular drug therapy. In order to predict this efficiency, one must first understand the transport of sodium and chloride through the membrane. This paper is directed at that question.

While the use of human cadaver skin *in vitro* for studying the passive diffusion of drugs across skin is firmly established (5), less is known about the utility of this technique for studying iontophoretic drug delivery. The use of skin which has been stored frozen poses the additional question of tissue integrity. In this study we have examined the properties of frozen, excised human skin and compared the results, where possible, to *in vivo* values.

MATERIALS AND METHODS

Materials

Human allograft skin (torso and thigh) was obtained from the Ohio Valley Skin and Tissue Center, Cincinnati, OH. The skin was obtained from cadavers with a dermatome set to 0.25 μm after the hair had been clipped and the skin washed. The skin was bathed in a solution of antibiotics for

[1] The Procter & Gamble Company, Miami Valley Laboratories, Cincinnati, Ohio 45239-8707.
[2] To whom correspondence should be addressed.

0724-8741/90/0200-0134$06.00/0

24 hr, then treated with a 10% glycerol solution (to retard ice crystal formation), packed in gauze and sealed aluminum foil packets, and slowly frozen to −150°C. The freezing rate was −1°C/min from room temperature to −40°C and −4°C/min from −40 to −90°C, after which the tissue was quickly placed in the vapor phase of a liquid nitrogen freezer. The slow cooling rate allowed water to escape from the cells during the freezing process, minimizing disruption of the tissue (6). After reception in our laboratory, the tissue was stored at −80°C for up to 2 months.

Prior to use, the skin was thawed by immersion in lukewarm water, rinsed with distilled water, and mounted in the diffusion cells with both sides immersed in a saline buffer. A thin layer of silicone grease (Dow Corning) was placed in the ground glass joint to ensure a perfect seal (7). Tests showed that this procedure did not appreciably affect the resistivity of the tissues.

^{22}NaCl, specific activity 58 Ci/mmol, radiochemical purity 99%, was obtained from NEN Research Products/Dupont Chemicals. The radiolabeled salt was diluted into the saline buffers to obtain final specific activities between 1.3 and 130 μCi/mmol. Dulbecco's phosphate-buffered saline (without calcium chloride and sodium bicarbonate), Tris base, Tris hydrochloride, sodium chloride, and sodium azide were purchased from Sigma Chemical Co. Distilled, deionized water was obtained from the building supply at Miami Valley Laboratories.

The buffer for Study 1, designated Buffer A, was Dulbecco's phosphate-buffered saline, pH 7.4, to which 0.02% (w/v) sodium azide had been added to retard microbial growth. The ionic composition was 156 m*M* Na^+, 141 m*M* Cl^-, 10 m*M* phosphate, 4.1 m*M* K^+, 3 m*M* N_3^-, and 0.5 m*M* Mg^+.

For Study 2, a 25 m*M* Tris · HCl buffer, pH 7.4 at 37°C, containing 0.02% sodium azide was prepared according to the manufacturer's specifications (1:2.62 ratio of Tris base to Tris · HCl). This solution was divided into three portions, and NaCl was added to each portion to yield solutions having Na^+ concentrations of 0.015 *M* (Buffer B), 0.147 *M* (Buffer C), and 1.59 *M* (Buffer D). Their electrical conductances and exact Na^+ concentrations were calculated from reference data (8).

Diffusion Cells and Electrical Circuitry

The apparatus has been described previously (9). The skin was clamped vertically in ground-glass joints (0.7 cm^2) with both sides immersed in a saline buffer and the stratum corneum facing the donor compartment. The volume of the donor and receptor compartments was 6 ml.

Current was supplied by means of silver wire electrodes coated with silver chloride and connected to a constant-current source. For the constant-voltage iontophoresis study, a low-voltage power source (Hewlett Packard 6286A, 0–20 V DC) was used in place of the normal 0- to 600-V supply. The potential difference across the skin was sensed potentiometrically using calomel electrodes (Fisher, radiometer type) and was corrected for the solution IR drop. The electrode response was highly linear (r^2 = 0.99999) over the current range of interest (9). Either a 1.5- or 6-V dry cell was used in the potentiometer circuit, depending on the magnitude of the signal being measured. The cells were magnetically stirred and maintained at 37 ± 2°C by means of heating, stirring modules. Sampling of the cells consisted of removing the entire receptor solution for radioactivity determination and replacing it with fresh buffer.

Experimental Protocol

Although the details differed, each study contained a similar sequence of procedures conducted over a period of 4 days. Table I shows a time line for both studies. The details of each procedure are given below.

Initial Resistance Measurements

After a 15- to 60-minute equilibration period in either Buffer A (for Study 1) or Buffer C (for Study 2), the potential difference across each cell was determined first with no applied current, then with a current, *I*, of 10 μA (or current density, *j*, of 14 μA/cm^2) imposed across the cell. The polarity was such that the epidermal side was positive with respect to the dermis. The resistance of the tissue at this current level [the "chord resistance" (10)] was calculated from Ohm's law. The corrections for zero offset and solution IR drop were 1–2% of the total signal. Two tissues in Study 1 which were obviously defective were replaced at this time.

Current–Voltage Measurements

Study 1. After initial resistance determination and a further equilibration period of 1–3 hr in Buffer A, short bursts of direct current of alternating polarity and increasing intensity were passed through each cell (n = 8) and the resulting potential differences determined. After the maximum intensity for a particular current regimen was reached, the magnitude of the current was reduced in the same stepwise manner. Three current regimens were consecutively imposed: 0 to ±10 μA in 2-μA steps, 0 to ±50 μA in 10-μA steps, and 0 to ±250 μA in 50-μA steps. For example, the sequence for the first regimen was 0, +2, −2, +4, −4 μA, etc. Alternate samples were tested with the negative polarity occurring first to avoid biasing the averages. Prior to each sequence the donor and receptor solutions were exchanged with fresh buffer. Completion of one sequence (20 readings) required about 10 min per sample. The flow of current was interrupted for about 5 sec with each polarity change to allow manual reversing of the leads. There was an overnight break following the 0 to ± 10 μA test regimen.

Study 2. After initial resistance determination and an overnight equilibration in Buffer C, null potentials (no applied current) were redetermined, the receptor solutions were exchanged with fresh Buffer C, and the donor compartments were rinsed and filled with either Buffer B, Buffer C,

Table I. Time Line for Experimental Procedures (Studies 1 and 2)

Day	Procedure
1	Mount skin; measure initial resistance
1–2	Current–voltage measurements
2–3	$^{22}Na^+$ passive diffusion
3–4	$^{22}Na^+$ iontophoresis

or Buffer D (n = 4 per formulation). The ascending portion of the current sequences from Study 1 was then applied to each cell. One cell was dropped from the study due to low resistivity.

Sodium Ion Transport Measurements

Study 1. Following completion of the current–voltage measurements, the receptor solution was exchanged with fresh Buffer A and the donor solution exchanged with Buffer A to which 0.44 μCi/ml of ^{22}NaCl had been added. The receptor compartments were sampled 2 and 17 hr postdose for radioactivity determination. The unidirectional sodium flux, J_{Na}, was calculated from the amount of radioactivity penetrated between 2 and 17 hr and the specific activity of $^{22}Na^+$ in the donor solution. Apparent sodium ion permeability coefficients, k_p, were calculated as

$$k_p = J_{Na}/C_v \tag{1}$$

where C_v is the sodium concentration in the donor solution.

Following the 17-hr sample, a constant direct current of 50 μA was passed across each cell for 6 hr, with the donor Ag/AgCl electrode serving as the anode. Periodic potential readings were obtained, and the receptor solutions removed for analysis at 2, 4, and 6 hr. The receptor current electrodes (cathodes) were then removed and recoated with AgCl by electrolysis in 1 *N* HCl.

On the following day a permeation sample was obtained, the pH of the donor solutions was lowered to 4.0 by the addition of 10.4 μl of 1 *N* HCl per ml of solution, and the iontophoresis procedure was repeated. Sodium ion membrane transference numbers (t_{Na}, the fraction of the electrical current carried by Na^+) were calculated for each time period from the relationship

$$t_{Na} = J_{Na}F/(3600j) \tag{2}$$

where J_{Na} is the unidirectional sodium flux expressed as μmol/cm^2 hr, F is the Faraday constant, and j is the electrical current density as μA/cm^2. This was a good approximation since the potential gradient in this study was sufficiently large that back-diffusion of ions against it should be negligible (4). The total amount of radioactivity penetrated during the 3 study days was 1–2% of the amount dosed.

An observed flux enhancement factor $J(v)/J(0)$ for each cell was calculated as the ratio of the average sodium flux between 2 and 6 hr during the pH 7.4 iontophoresis treatment to the passive diffusion flux. These values were compared to the theoretical value for an uncharged homogeneous membrane immersed in solutions of identical composition (4):

$$J(v)/J(0) = v/[1 - \exp(-v)] \tag{3}$$

The parameter v was calculated for each cell as

$$v = zF\langle V\rangle/RT \tag{4}$$

where $z = +1$, R is the gas constant, T is the absolute temperature, and $\langle V\rangle$ is the time-averaged potential difference across the skin between 2 and 6 hr. Average potential drift during this period was 6% (range, 2–13%) of the initial value.

Study 2. Following the current–voltage measurements, the receptor solutions were exchanged with fresh Buffer C and the donor solutions were exchanged with Buffer B, C, or D to which 2 μCi/ml of ^{22}NaCl had been added. Passive permeation samples were obtained at 2, 4, 6, and 23 hr postdose. Periodic potential measurements were made in order to follow the development of diffusion potentials caused by the unequal salt concentrations in the cells. Passive unidirectional sodium ion flux and permeability coefficients were calculated as in Study 1 from the amount of radioactivity penetrated between 6 and 23 hr.

After 24 hr three constant-voltage regimens, consisting of target voltages of 57, 114, and 171 mV, were applied consecutively to each cell. Constant voltage on our apparatus was approximated by periodically adjusting the current source so as to maintain the desired potential difference across the skin. Each target voltage was applied for 3 hr. Permeation samples were obtained hourly, and frequent current and voltage readings were made. Unidirectional sodium ion flux and observed active/passive flux enhancement factors were calculated for each time period, as was the ratio of the unidirectional flux to the total electrical current. The latter value should not be interpreted as an electrical transference number in this study since it included both an electrogenic (charge-carrying) and a nonelectrogenic component due to the salt concentration gradient, and, furthermore, the applied potentials were not large enough to prevent back-diffusion of ions. Nevertheless, it was an experimentally observable ratio which could be compared with theoretical predictions.

The observed flux enhancement factors were compared with the values expected for an uncharged homogeneous membrane under the electroneutrality approximation (4):

$$\frac{J(v)}{J(v_o)} = \left(\frac{\ln\chi + v}{\ln\chi + v_o}\right)\left[\frac{\chi - \exp(-v_o)}{\chi - \exp(-v)}\right] \tag{5}$$

In Eq. (5), χ is the ratio of the total ion concentration in the donor solution to that in the receptor solution, v is the driving force defined in Eq. (4), and $v_o = zF\langle V_0\rangle/RT$, where $\langle V_0\rangle$ is the time-averaged diffusion potential present during passive diffusion.

Observed sodium flux/current ratios were calculated according to Eq. (2). They were compared to an approximate calculation from the electroneutrality model (4) resulting from the assumption that all current through the membrane was carried by either sodium or chloride ions:

$$t_1^{calc} = \left(\left(1 - \frac{c_{10}}{c_{1h}}\right)\left\{1 + \frac{D_2}{D_1}\left[\frac{\ln(\xi/\chi)}{\ln(\chi\xi)}\right]\left(\frac{\chi\xi - 1}{\chi - \xi}\right)\left(\frac{c_{2h} - \xi c_{20}}{\xi c_{1h} - c_{10}}\right)\right\}\right)^{-1} \tag{6}$$

In Eq. (6), subscript 1 refers to sodium ion and 2 to chloride, c_{ih} is the concentration of species i in the donor solution, c_{i0} is its concentration in the receptor solution, and $\xi = \exp(-v)$. D_2/D_1 is the ratio of chloride to sodium ion diffusivities (or mobilities) in the membrane. Since all the parameters in Eq. (6) were known except for D_2/D_1, this equation was useful for estimating the diffusivity ratio in the model which would lead to the observed flux/current ratios.

Assay for Penetration

Sodium transport through the skin was assessed by determining the total amount of radioactivity accumulated in the receptor solutions. The gamma radiation resulting from the decay of ^{22}Na was measured using a Packard Auto-Gamma 5530 counter with a counting efficiency of 41% for ^{22}Na and a counting time of 10 min per sample.

RESULTS

Skin Resistance and Sodium Ion Permeability Coefficients

The initial resistance values of the skin samples from Studies 1 and 2 and a third study conducted similarly are shown in Table II. Sodium ion permeability coefficients for Studies 1 and 2 are also shown (they were not determined in the third study). Most of the samples were highly resistive, having effective resistances under the test conditions of 20–200 kΩ, corresponding to specific resistances (resistance × area) of 14–140 kΩ cm^2. For reasons described in the following section, those samples with resistances in the range 20–50 kΩ were considered to be marginal, and those with $R < 20$ kΩ were considered unusable. Nevertheless, more than three-fourths of the samples mounted in these studies exceeded the 50-kΩ (35-kΩ cm^2) criterion. This was an improvement over an earlier study utilizing this skin preparation (9), where only 4 of 12 samples tested similarly met this criterion. Length of storage of the excised tissue may be critical: we observed dramatic decreases in the resistivity of samples stored at −80°C for greater than 2 months (data not shown).

While high, these resistance values are lower than those reported by Tregear (11) for human forearm skin *in vivo*. Using a low-frequency AC technique with a driving potential of 1 V rms, Tregear obtained a mean specific impedance of 880 kΩ cm^2 (range, 590–1170) for skin in contact with a normal saline solution. Although some of the difference may be due to test conditions, it seems likely that the excised skin was less resistive than human skin *in vivo*.

Table II. Initial Resistance and Sodium Ion Permeability Coefficients for Excised Human Skin *in Vitro*

R^e (kΩ)	$k_p^f \times 10^6$ (cm/min)	R^e (kΩ)	$k_p^f \times 10^6$ (cm/min)	R^e (kΩ)	$k_p^f \times 10^6$ (cm/min)
197	0.20[d]	150	0.41[b]	80	1.01[a]
192	0.17[a]	148		72	0.92[c]
168	0.63[b]	148	6.08[c]	53	
167	0.31[c]	127		43	1.03[a]
167	0.45[a]	127		42	0.55[d]
166	0.10[d]	124	0.90[a]	34	
>150		118	0.76[d]	28	
>150		98	13.42[a]	21	19.87[b]
>150		91	1.08[a]	<20	
>150		88	0.84[a]	3.5	
>150		82	2.13[b]	1.6	
>150					

[a] Donor Solution A (0.156 *M* Na^+).
[b] Donor Solution B (0.015 *M* Na^+).
[c] Donor Solution C (0.147 *M* Na^+).
[d] Donor Solution D (1.59 *M* Na^+).
[e] Effective resistance at 10 μA of 0.7-cm^2 samples (j = 14 μA/cm^2).
[f] Passive permeability determined prior to iontophoresis.

The sodium ion permeability coefficients showed a better agreement with *in vivo* values. In another study (12), Tregear reported the permeability coefficient for sodium ion through human forearm skin *in vivo* to be 0.6–1.0 × 10^{-6} cm/min. Most of the values in Table II fall within this range or lower. We have no explanation for the three samples with normal initial resistance but anomalously high k_p values. With the exception of these samples, there was a strong inverse correlation between k_p and initial resistance, as shown in Fig. 1. Surprisingly, the plot of k_p versus resistance was more linear than that versus conductance (the inverse of resistance). However, a subsequent study in which the expected proportionality to conductance was observed indicated that this result could be attributed to resistivity changes in the tissue following the initial resistance determination (13). In the latter study a much tighter relationship was demonstrated between k_p and tissue conductance measured immediately after the permeability measurements.

Current–Voltage Characteristic for Skin in Normal Saline Solutions

Figures 2 and 3 show the mean current–voltage relationship observed for the skin samples in Study 1. The curves were nonlinear and slightly asymmetric with respect to the sign of the applied potential. As the magnitude of the current increased, the transient time for reaching stable potential readings also increased. For the 0- to ±10-μA current regimen (Fig. 2a), the voltage was quite stable after 5–10 sec, and there was little evidence for the production of irreversible or slowly reversible changes in the skin. This follows from the minimal amount of hysteresis evident in the figure, i.e., potentials measured during the descending current sequence closely matched those on the ascending sequence. Longer transient times and increasing amounts of hysteresis were seen in the 0- to ±50- and 0- to ±250-μA regimens (Figs. 2b and c). Rather than waiting to achieve stable potential readings for these ranges, which would have required

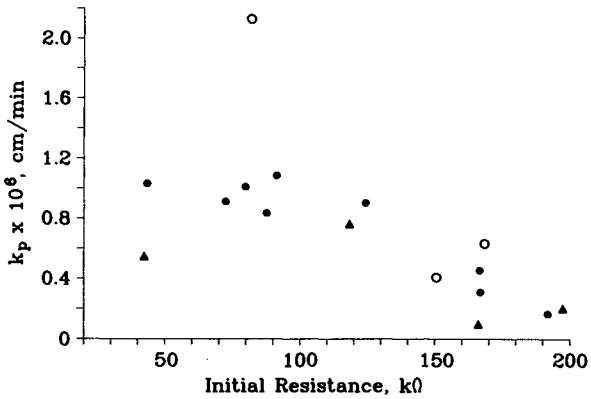

Fig. 1. Sodium ion permeability coefficients of excised human skin samples (0.7 cm^2) versus their initial resistance at a current of 10 μA. Donor solution sodium ion concentrations were either 0.015 *M* (open circles), 0.15 *M* (filled circles), or 1.59 *M* (filled triangles). Permeability was determined following the current–voltage measurements but prior to sustained iontophoresis.

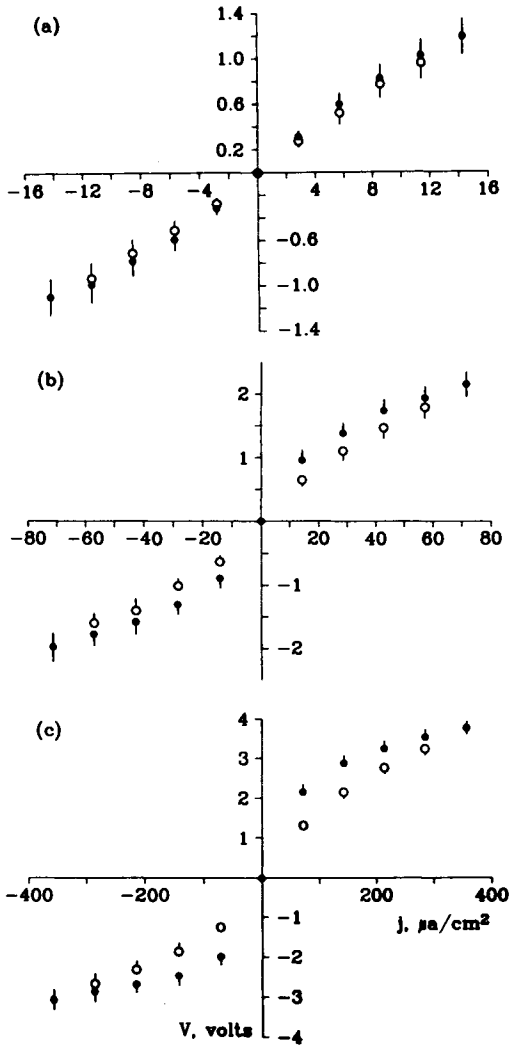

Fig. 2. Mean current–voltage characteristic (n = 7) for human skin samples immersed in a normal saline buffer. Data obtained with increasing current magnitude are drawn as filled circles; those with decreasing current magnitude as open circles. The error bars are 1 SE. (a) 0 to ±10 μA regimen; (b) 0 to ±50 μA regimen; (c) 0- to ± 250-μA regimen.

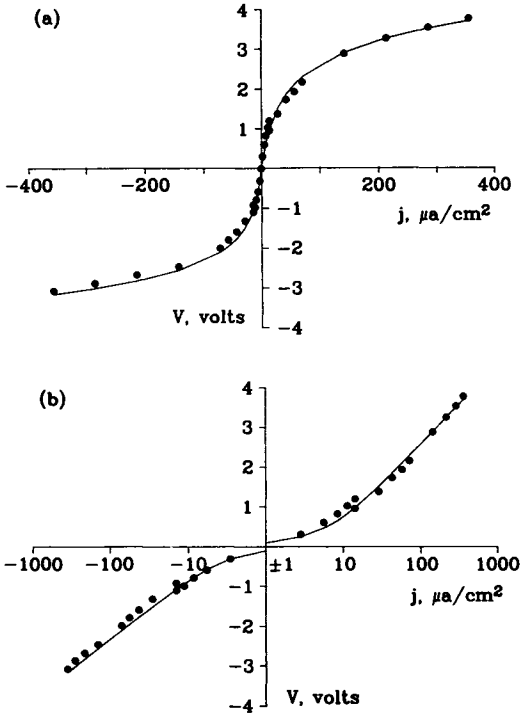

Fig. 3. Ascending current–voltage data from Fig. 2 plotted with (a) a linear current axis or (b) a logarithmic current axis. The smooth curves are calculated according to Eq. (7), using the parameters in the last two rows in Table IV.

tens of minutes per reading for the 0- to ±250-μA range, we chose to record the potential after 15–20 sec and then move to the next current setting; thus, the shape of the j–V curve and the size of the hysteresis loop measured for these current ranges is related to the speed with which the measurements were made. The use of longer equilibration times would have led to even greater nonlinearities, since the potential drifted toward lower absolute values as the magnitude of the current increased.

The potential drift was not always in the direction of decreasing skin resistance. On the descending arm of the j–V cycles, the potentials actually increased with time. Figure 4 shows an example of this phenomenon. The time scale for the recovery of resistance was longer than that for resistance loss, and the recovery was not complete. However, Table III shows that greater than 80% of the initial sample resistance for each current sequence was recovered after 1–2 hr.

The ascending data from all three current ranges are plotted together in Fig. 3. The data were nearly linearized by a logarithmic transformation of the current axis (Fig. 3b). This type of behavior is characteristic of systems containing potential-dependent barriers to charge or mass transport (14). The shape of the curves was satisfactorily described by the following relationship:

$$V = (4aRT/F)\sinh^{-1}(bj) \qquad (7)$$

where a and b are adjustable parameters and the other quantities have been described previously. The equation is written as shown for comparison with the predictions of ionic mass transport theories incorporating kinetic limitations. In one such theory (15), the parameter a is equal to the number of barriers within the membrane which each ion must cross and b is the sum of the rate constants for traversing the barrier. However, for the present purposes, Eq. (7) may be regarded as a phenomenological means of characterizing the data.

The parameters a and b in Eq. (7) were determined for each sample using standard nonlinear regression techniques (16), and the results averaged. Table IV shows the results of the fitting procedure. The fitted parameters were similar whether the three current ranges were fit together or separately. Deviations of the data from the fitted curves (as measured by the mean squared residuals) increased as the magnitude of the current increased. There were small, but significant differences between the fitted parameters for positive and negative polarities, as determined by an F test on the ratios of the residuals.

One of the eight samples tested was omitted from the results. This sample had an initial resistance of 43 kΩ, while the others exceeded 80 kΩ. The lower resistance sample had

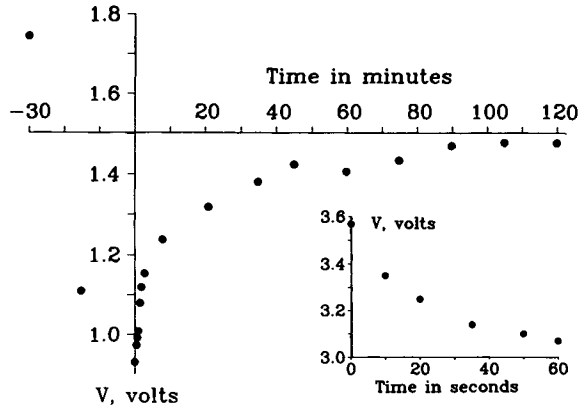

Fig. 4. Loss and recovery of resistance in a skin sample subjected to 50 μA for 1 min and then tested periodically at a current of 10 μA. The ordinate is the measured potential drop across the skin. The resistance loss at 50 μA was nearly complete in 1 min (inset), whereas the recovery took approximately 90 min. The points to the left of $t = 0$ represent the potential drop at 10 μA at the start and finish of the 0 to ±50 μA current regimen, which was conducted immediately prior to the 1-min exposure.

a more linear j–V characteristic than the others, although not nearly as linear as several samples of expired skin having much lower resistance values which were studied in a separate experiment (data not shown). The transitional nature of the j–V curve for this sample, in combination with the sodium ion permeability data in Table II, forms the basis for the recommendation of a 50-kΩ (35-kΩ cm^2) resistance cutoff for *in vitro* skin samples.

Sodium Ion Transference Number and Enhancement Factor in Normal Saline During Iontophoresis at 50 μA

Table V shows the membrane transference numbers (t_{Na}) for sodium ion during the iontophoresis portion of Study 1. There was a time lag evident in the attainment of steady-state sodium flux at pH 7.4, as measured by radioactivity accumulation in the receptor phase. This may reflect a period during which the membrane was being loaded with $^{22}Na^+$ from the donor solution, rather than an actual change in sodium flux or transference number. The mean value of t_{Na} from 2 to 6 hr was 0.51 at pH 7.4 and 0.24 at pH 4.0. The pH 7.4 value was less than the value $t_{Na} = 0.62$ determined by Burnette and Ongpipattanakul (17) in a similar experiment using freshly excised human thigh skin. Since the concentration of cations other than sodium in our system was very low, it is evident that our tissues were less cation-selective than those of Burnette. Nevertheless, some permselectivity was obtained, since the transference number for Na^+ in normal saline is about 0.4 (17).

The substantial drop in the value of t_{Na} when the donor solution pH was lowered from 7.4 to 4.0 may be due to one or both of the following factors. (1) The negative charge on the skin would be reduced at the lower pH, favoring the transport of chloride ions versus sodium ions; and (2) much higher concentrations of hydronium ion are present at pH 4. Although still much lower in concentration than Na^+, H_3O^+ has an anomalously high mobility in solution (18) and may have an even higher relative mobility in the membrane. However, its mobility relative to sodium ion would have to be extremely high (>3000) for the second factor to account completely for the observed effect.

Table VI compares the sodium ion flux at a current of 50 μA with that observed during passive diffusion. The active flux values are much more consistent than the passive values, reflecting the fact that constant current iontophoresis constrains the total ion current to a fixed value, forcing the flux of major charge carriers like Na^+ and Cl^- to be relatively constant. (The same does not follow for minor charge carriers having low mobilities in the membrane.) Also shown in Table VI are the observed iontophoretic enhancement factors and those calculated from Eqs. (3) and (4) using the measured potential differences across the skin. The observed enhancement factors were generally three to five times greater than the calculated values. This is consistent with the fact that the membrane resistances were substantially reduced at the 50-μA current level relative to their

Table III. Loss and Recovery of Resistance in Skin Following Current–Voltage Studies

Current regimen	Mean ± SD (n = 7)	Range
0 to ±10 μA		
Initial PD at I = 2 μA (V)	0.32 ± 0.14	0.18–0.56
% of initial PD posttreatment	87 ± 18	58–109
% of initial PD following recovery period[a]	ND[b]	ND
0 to ±50 μA		
Initial PD at I = 10 μA (V)	0.96 ± 0.46	0.61–1.74
% of initial PD posttreatment	70 ± 8	57–80
% of initial PD following recovery period[a]	85 ± 3	81–89
0 to ±250 μA		
Initial PD at I = 50 μA (V)	2.16 ± 0.49	1.75–3.11
% of initial PD posttreatment	61 ± 3	57–65
% of initial PD following recovery period[a]	82 ± 3	79–88

[a] Recovery period was 1–2 hr.
[b] Not determined.

Table IV. Results of Fitting Eq. (7) to the Current–Voltage Data in Figs. 2 and 3

Data set	No. of points	Mean parameter value ± SD[a] a	Mean parameter value ± SD[a] log b^b	MSR[c]
Fig. 2, ascending data only				
−14 to +14 μA/cm^2	11	9.3 ± 4.2	−0.90 ± 0.14	0.0016
−71 to +71 μA/cm^2	11	7.9 ± 2.2	−0.98 ± 0.24	0.0109
−360 to +360 μA/cm^2	11	8.3 ± 1.3	−1.04 ± 0.19	0.1362
Fig. 3				
All data	33	7.6 ± 1.5	−0.91 ± 0.34	0.0521
$I \geq 0$	18	8.8 ± 1.0	−1.02 ± 0.29	0.0183
$I \leq 0$	18	6.6 ± 2.0	−0.76 ± 0.46	0.0086

[a] Mean and standard deviation for seven tissue samples.
[b] Units of b are cm^2/μA.
[c] Mean squared residuals in fit (V^2).

Table V. Sodium Ion Transference Numbers During Constant-Current Iontophoresis (I = 50 μA) in Normal Saline Buffer

pH	Time (hr)	t_{Na}, mean ± SD (n = 8)
7.4	0–2	0.39 ± 0.05
	2–4	0.50 ± 0.06
	4–6	0.53 ± 0.04
	2- to 6-hr average	0.51 ± 0.05
4.0	0–2	0.26 ± 0.05
	2–4	0.23 ± 0.08
	4–6	0.25 ± 0.04
	2- to 6-hr average	0.24 ± 0.02

values during passive diffusion, whereas Eq. (3) follows from the assumption of constant membrane properties (4).

Current–Voltage Characteristic for Skin in the Concentration Study

Figure 5 shows the current–voltage relationship for the skin samples subjected to unequal salt concentrations on opposite sides of the membrane (Study 2). The curves were qualitatively similar to those obtained in the first study. Although the model leading to Eq. (7) does not give a simple closed-form solution for the case of unequal salt concentrations (19), this form was adequate to phenomenologically characterize the curves. Table VII shows the results. As in Study 1, an asymmetry between positive and negative arcs of the j–V curve was evident at two of the three concentrations studied. In each case the asymmetry was in the same direction: with the epidermal side positive with respect to the dermis, the samples were more conductive at low currents and less conductive at high currents than with the potential reversed. In terms of Eq. (7), this means that the positive arm was characterized by a higher value of a and a lower value of b.

The three remaining samples from Study 2 had a much lower resistivity and yielded bilinear j–V characteristics. Such a form is expected for homogeneous membranes bathed in solutions of differing compositions (4). These samples were not included in the analysis, as the integrity of the membranes was believed to be compromised.

Diffusion Potential and Sodium Ion Flux in Concentration Study

Measurable diffusion potentials developed slowly in the samples subjected to unequal salt concentrations. The evolution of these potentials is shown in Fig. 6. Samples having a lower salt concentration in the donor compartment (epidermal side) developed positive diffusion potentials, i.e., the donor solution was positive with respect to the receptor solution. Samples having a higher salt concentration in the donor compartment developed negative potentials. The sign of these potentials is consistent with the concept that the membranes were permselective for sodium ion versus chloride (4). Their magnitude actually suggests a much greater degree of permselectivity than do the transference number calculations, based on approximate calculations using the electroneutrality model (4). This could (it seems to us) be a consequence of the net negative charge on skin.

Steady-state unidirectional sodium ion flux values obtained during the passive diffusion stage of this study are shown in Table VIII. These values were divided by the sodium concentration in the donor phase to give the permeability coefficients in Table II. No evidence for a non-Fickian dependence of flux on concentration was evident in this small sample; however, substantially more data would be required to establish this firmly.

Sodium Ion Enhancement Factors and Transference Numbers During Constant-Voltage Iontophoresis

Following the passive diffusion measurements, the samples from Study 2 were subjected to three iontophoresis treatments, during which an attempt was made to maintain the potential across the skin at 57, 114, and 171 mV. The

Table VI. Theoretical and Observed Enhancement Factors for Sodium Ion Flux During Constant-Current Iontophoresis at 50 μA[a]

Cell ID	Sodium ion flux (nmol cm^{-2} hr^{-1})		$\langle V \rangle$ ± SD[b] (V)	Active/passive enhancement factor		
	Passive[c]	Active[d]		Observed	Theory[e]	Ratio
1	125.6	1390	1.06 ± 0.03	11	42	0.3
2	9.4	1480	1.30 ± 0.01	157	52	3.0
3	4.2	1340	1.48 ± 0.06	317	59	5.3
4	1.6	1070	1.55 ± 0.10	683	62	11.0
5	8.5	1360	1.39 ± 0.01	160	55	2.9
6	7.8	1380	1.37 ± 0.05	176	55	3.2
7	10.1	1520	1.09 ± 0.02	150	44	3.5
8	9.7	1420	1.30 ± 0.02	146	52	2.8
				Geometric mean ± SD[f]		$4.0^{+2.6}_{-1.6}$

[a] All data are from Study 1 and were determined in Buffer A.
[b] Potential difference across skin from 2 to 6 hr during iontophoresis treatment at pH 7.4
[c] Determined overnight immediately preceding iontophoresis treatment.
[d] Average flux from 2 to 6 hr during iontophoresis treatment.
[e] Calculated according to Eqs. (3) and (4).
[f] Calculated omitting the value for Cell 1.

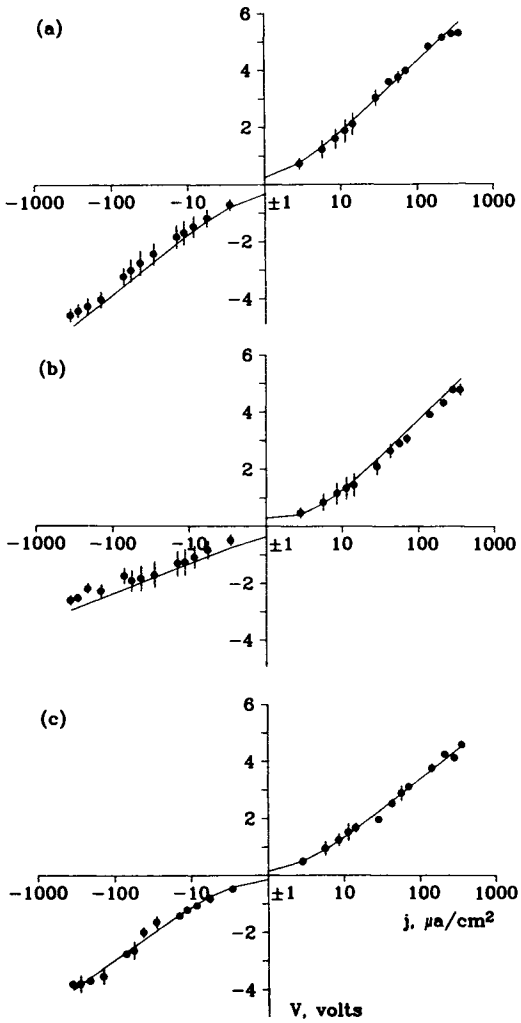

Fig. 5. Mean current–voltage relationship for skin samples in Study 2. The error bars are ±1 SE, and the smooth curves are calculated using Eq. (7) and the parameters listed in Table VII. The donor solution sodium ion concentrations were (a) 0.015 M (n = 3), (b) 0.147 M (n = 3), and (c) 1.59 M (n = 2). The receptor solution contained 0.147 M Na^+ in all cases.

Table VII. Results of Fitting Eq. (7) to the Current–Voltage Data in Fig. 5

Data set	No. of points	Mean parameter value ± SD: a	Mean parameter value ± SD: log b^a	MSR[b]
Donor solution B (0.015 M Na^+; n = 3)				
All data	28	10.0 ± 2.5	−0.53 ± 0.47	0.1356
$I \geq 0$	14	10.8 ± 2.2	−0.55 ± 0.38	0.0371
$I \leq 0$	14	9.2 ± 3.1	−0.51 ± 0.61	0.0154
Donor solution C (0.147 M Na^+; n = 3)				
All data	28	7.8 ± 2.7	−0.59 ± 0.72	0.4283
$I \geq 0$	14	11.2 ± 3.8	−0.83 ± 0.53	0.0116
$I \leq 0$	14	4.6 ± 1.5	−0.12 ± 1.10	0.0387
Donor solution D (1.59 M Na^+; n = 2)				
All data	28	8.7 ± 0.3	−0.72 ± 0.10	0.0765
$I \geq 0$	14	9.1 ± 0.8	−0.68 ± 0.19	0.0302
$I \leq 0$	14	8.3 ± 0.3	−0.76 ± 0.01	0.0572

[a] Units of b are $cm^2/\mu A$.
[b] Mean squared residuals in fit (V^2).

mean potentials (±SD) actually obtained for the six samples which were usable for this phase of the study (as judged by tissue resistance and Na^+ transport) were 54 ± 3, 109 ± 3, and 169 ± 6 mV. Samples with a low conductivity yielded more stable potential readings than those with a high conductivity, perhaps because they suffered fewer current-induced physical changes.

Hourly sodium ion transport measurements showed that steady-state flux was generally not achieved during the 3-hr duration of each treatment. In five of the six samples the flux was still increasing after 3 hr, although the current levels were steady; however, the declining rate of increase was indicative of an approach to steady state. Based on this observation, approximate iontophoretic enhancement factors were calculated at each value of the potential, using the 2- to 3-hr flux as an estimate of the steady-state value. The results are shown in Table VIII, along with the predicted values calculated from Eq. (5). For the samples tested with Donor Solutions A and B, the observed and calculated enhancement factors were in good agreement; however, the samples tested with Donor Solution C had observed enhancements two to five times greater than the calculated values. It seems worth noting that the constant field approximation, Eq. (3), gives somewhat better agreement with the data than does Eq. (5), since the enhancement does not fall off at high donor concentrations under this approximation. However, more work is required to verify the agreement with either theory. It seems likely that the generally better agreement of the data in Table VIII with the homogeneous membrane theories compared to those in Table VI reflects the much lower power levels used in the constant-voltage study, leading to fewer alterations in skin properties.

The ratio of the unidirectional sodium ion flux to the total electrical current during the constant-voltage iontophoresis study is shown in Table IX. At the 169-mV potential, this ratio is essentially equal to the sodium ion transference number, since the backflow of ions against the potential gradient may be neglected (4). At lower potentials, a substantial component of nonelectrogenic salt transport is in-

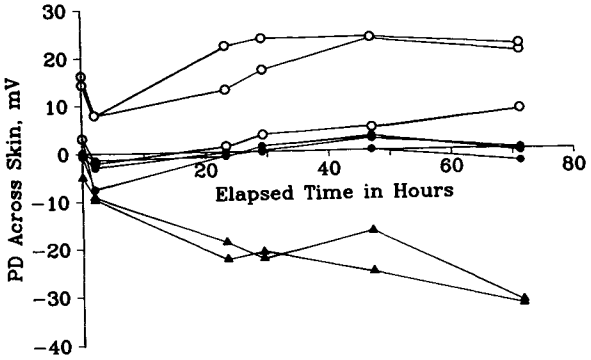

Fig. 6. Diffusion potentials for skin samples tested in Study 2. Donor solution sodium ion concentrations were either 0.015 M (open circles), 0.147 M (filled circles), or 1.59 M (filled triangles).

Table VIII. Theoretical and Observed Enhancement Factors for Sodium Ion Flux During Constant-Voltage Iontophoresis Experiment

Cell ID	$[Na^+]$ (M)	χ	J_0 (nmol/cm^2 hr)	V_0 (mV)	Enhancement factor $J(v)/J(v_0)$ 54 mV Obs.	54 mV Calc.	109 mV Obs.	109 mV Calc.	169 mV Obs.	169 mV Calc.
1	0.015	0.20	0.4	18	2.7	2.1	4.3	4.7	6.7	8.3
2			1.9	3	2.6	3.0	4.4	6.8	7.9	11.9
3			0.6	23	—[a]	1.9	—[a]	4.2	—[a]	7.4
4	0.147	1.00	2.7	0	2.8	2.4	4.7	4.4	6.9	6.8
5			8.1	1	3.8	2.4	4.9	4.3	6.8	6.6
6			66.0	−1	—[a]	2.5	—[a]	4.5	—[a]	6.9
7	1.59	9.77	19.2	−23	9.9	2.5	17.2	3.6	15.0	4.9
8			9.2	−25	9.8	2.5	10.3	3.8	8.7	5.1

[a] Anomalous flux after passive flux determination.

cluded. Because the measured sodium flux increased faster than the current, the observed flux/current ratios also tended to increase with time; the values reported are those from 2 to 3 hr. They are compared with the approximate values calculated from Eq. (6). A mobility ratio $D_{Cl}/D_{Na} = 1$ gave the best agreement with the observed values.

DISCUSSION

Frozen, excised human skin obtained from skin banks has received widespread use in skin penetration studies. Franz (20) and others have shown that such tissue can give drug permeation rates which are comparable to those obtained with fresh skin *in vitro* and to the results of human *in vivo* studies. Less is known about the utility of this tissue for studying the permeation of ions. Since ionic penetration rates through skin are extremely low, it seemed possible that defects induced by the freezing process might grossly alter the permeability of the tissue to ions, rendering it useless for such studies.

The data reported here indicate that it may well be useful. Although the resistivity of the tissue was not as great as that of human skin *in vivo,* the majority of tissue samples mounted in these studies had specific resistances at 10 μA of $\geq$35 kΩ cm^2 and sodium ion permeability coefficients comparable to human *in vivo* values. By prescreening samples to meet this resistance criterion, it should be possible to obtain reliable ionic permeation data from frozen, excised skin.

The tissue used in our studies was carefully treated to minimize the effects of freezing. The key features in its preparation were believed to be the incorporation of glycerol into the freezing solution, the slow, programmed freezing rate, and limitation of the storage time while frozen (6). The use of alternative freezing methods may well give different results.

The DC current–voltage relationship for the skin samples tested was strongly nonlinear, showing a decrease in resistance with increasing values of the current. This decrease was either wholly or partially reversible, depending on the magnitude of the current. Such behavior is not compatible with homogeneous membrane theories of ionic transport in which equilibrium is maintained at the membrane–solution interfaces (4). It is reminiscent of the current–voltage behavior obtained at many electrode–solution interfaces (14); consequently, it may be possible to explain the shape of the curves by theories involving restricted interfacial charge transport (15). Equation (7), which stems from a theory of this sort, provided a satisfactory fit to the data.

Diffusion potentials, sodium ion transference numbers, and iontophoretic enhancement factors were also determined in these studies. Sodium ion transference numbers of about 0.51 in normal saline, combined with the sign of the diffusion potentials in the concentration study, provide evidence for a weak permselectivity of skin for sodium ion versus chloride. This result supports the findings of Burnette

Table IX. Ratio of Unidirectional Sodium Flux to Total Electrical Current During Constant-Voltage Iontophoresis Experiment

Cell ID[a]	$[Na^+]$ (M)	χ	Flux/current ratio 54 mV Obs.	54 mV Calc.[b]	109 mV Obs.	109 mV Calc.	169 mV Obs.	169 mV Calc.
1	0.015	0.20	0.19	0.16	0.10	0.19	0.08	0.22
2			0.16		0.13		0.26	
4	0.147	1.00	0.46	0.54	0.36	0.48	0.34	0.48
5			0.61		0.41		0.35	
7	1.59	9.77	1.95	1.04	1.77	0.76	0.69	0.67
8			1.70		1.08		0.47	

[a] Cells 3 and 6 omitted due to anomalous flux values.
[b] Calculated according to Eq. (6) with $D_2/D_1 = 1$.

and Ongpipattanakul (17), although the degree of permselectivity may be less in the present study.

The discrepancy between the sodium ion enhancement factors observed in the constant-current iontophoresis study and the predictions of the homogeneous membrane theory can be accounted for by the current–voltage data. Declining membrane resistance with increasing potential across the skin leads to sodium fluxes and total electrical current which increase faster with increasing potential than predicted by the theory. At the very low potential levels used in the constant-voltage study, the agreement was better but still incomplete. More data are required for a quantitative comparison under these conditions.

CONCLUSIONS

Frozen, excised human skin has been shown to be a promising tissue for conducting iontophoresis studies, provided the tissue is properly prepared and electrically prescreened for defects. Ionic transport in this tissue cannot be adequately predicted by theories involving an uncharged, homogeneous membrane with equilibrium boundary conditions. A theory incorporating kinetic barriers to charge transport may better explain the observed phenomena.

ACKNOWLEDGMENTS

The authors would like to thank R. M. Deibel and G. O. Kinnett for their help with the radioactivity studies and R. T. Plessinger for his helpful comments concerning preparation of the skin.

REFERENCES

1. A. K. Banga and Y. W. Chien. *J. Control. Release* 7:1–24 (1988).
2. R. R. Burnette and D. Marrero. *J. Pharm. Sci.* 75:738–743 (1986).
3. B. R. Meyer, W. Kreis, J. Eshbach, V. O'Mara, S. Rosen, and D. Sibalis. *Clin. Pharmacol. Ther.* 44:607–612 (1988).
4. G. B. Kasting and J. C. Keister. *J. Control. Release* 8:195–210 (1989).
5. R. J. Scheuplein. In A. Jarrett (ed.), *The Physiology and Pathophysiology of the Skin, Vol. 5,* Academic Press, London, 1978, pp. 1659–1752.
6. R. T. Plessinger. Personal communication, Ohio Valley Skin and Tissue Center.
7. J. Ostrenga, C. Steinmetz, and B. Poulson. *J. Pharm. Sci.* 60:1175–1179 (1971).
8. R. C. Weast (ed.). *Handbook of Chemistry and Physics,* 62nd ed., CRC Press, Boca Raton, FL, 1981, p. D-232.
9. G. B. Kasting, E. W. Merritt, and J. C. Keister. *J. Membrane Sci.* 35:137–159 (1988).
10. A. Finklestein and A. Mauro. In *Handbook of Physiology, Section 1: The Nervous System, Vol. I,* Am. Physiol. Soc., Bethesda, MD, 1977, Chap. 6, pp. 161–213.
11. R. T. Tregear. *Nature* 205:600–601 (1965).
12. R. T. Tregear. *J. Invest. Dermatol.* 46:16–23 (1966).
13. G. B. Kasting and L. A. Bowman. In preparation.
14. A. J. Bard and L. R. Faulkner. *Electrochemical Methods: Fundamentals and Applications,* Wiley, New York, 1980, pp. 87–118.
15. J. C. Keister and G. B. Kasting. The mechanism of iontophoresis, Proceedings of NIH conference on physical and chemical enhancement of drug transport through skin, Bethesda, MD, May 23–24, 1988.
16. P. R. Bevington. *Data Analysis for the Physical Sciences,* McGraw–Hill, New York, 1969, p. 235 (Marquardt algorithm).
17. R. R. Burnette and B. Ongpipattanakul. *J. Pharm. Sci.* 76:765–773 (1987).
18. R. C. Weast (ed.). *Handbook of Chemistry and Physics,* 65th ed., CRC Press, Boca Raton, FL, 1984, pp. D171–D173.
19. J. C. Keister and G. B. Kasting. Unpublished results.
20. T. J. Franz. *J. Invest. Dermatol.* 64:190–195 (1975).